

# Chapter 19

## Safety

*T. Otto*<sup>1\*</sup>, *C. Adorisio*<sup>1</sup>, *C. Gaignant*<sup>1</sup>, *A. Infantino*<sup>1\*</sup> and *M. Maietta*<sup>1</sup>

<sup>1</sup>CERN, Accelerator & Technology Sector, Switzerland

\*Corresponding authors

### 19 Safety

#### 19.1 Overview

CERN declares in its Safety Policy [1] that it will ensure the best possible protection in health and safety matters of all persons participating in the Organization's activities or present on its site, as well as of the population living in the vicinity of its installations, limit the impact of the Organization's activities on the environment, and guarantee the use of best practice in matters of Safety.

A safety organisation accompanies the life cycle of every large project, such as the HL-LHC, to ensure that the Organization's Safety objectives are met. This Chapter describes the safety assessment process applied to the deliverables of the HL-LHC project. As the methods to achieve the safety objectives differ between occupational and operational Safety and Radiation Protection (RP), the two subjects are treated in distinct Subsections.

#### 19.2 Radiation protection considerations

##### 19.2.1 Design constraints and the "As Low As Reasonably Achievable" (ALARA) principle

Design constraints for new or upgraded facilities should ensure that the exposure of persons working on CERN sites, the public, and the environment will remain below the specified dose limits [2] under normal as well as abnormal conditions of operation, and that the optimization principle is implemented [3][4]. In particular, the following design constraints apply:

- The design of components and equipment must be optimized such that installation, maintenance, repair, and dismantling work does not lead to an effective dose, e.g. as calculated with Monte Carlo simulations, exceeding 2 mSv per person and per intervention. The design is to be revised if the dose estimate exceeds this value for cooling times compatible with operational scenarios.
- The annual effective dose to any member of a reference group outside of the CERN boundaries must not exceed 10  $\mu$ Sv. The estimate must include all exposure pathways and all contributing facilities.
- The selection of construction material must consider activation properties to optimize dose to personnel and to minimize the production of radioactive waste. In order to guide the user, a web-based code (ActiWiz) is available for CERN accelerators [5].

Proton-proton collisions in the LHC experiments produce a secondary radiation field that penetrates into the adjacent accelerator tunnels and can cause severe activation of beam-line elements. Consequently, in such areas the design of components and infrastructure has to be optimized to follow the As Low As Reasonably Achievable (ALARA) principle. The optimization of the design for later interventions is an

iterative process: dose equivalent maps per unit time of exposure (called dose rate maps below) of the concerned area(s) are compiled from measurements and/or simulations with Monte Carlo particle transport codes such as FLUKA [6][7]. Based on these maps, the individual and collective doses of the intervention teams are calculated by using an intervention plan that then allows identification of and optimization of critical work steps in order to reduce doses to intervening personnel. If the latter involves a change in design or work scenario, then doses are re-evaluated by repeating the above steps.

### 19.2.2 Residual dose rate predictions for the Long Straight sections in Point 1 and 5

Residual dose rate maps were calculated with FLUKA for the part of the Long Straight Sections (LSS) in Point 1 (P1) and 5 (P5) that extend from the Target Absorber Secondary (TAXS) up to quadrupole Q7 in Cell 7, according to the latest HL-LHC layout (optic v1.5). Activation in LSS1 and LSS5 is dominated by the debris coming from p-p collisions at 14 TeV centre-of-mass energy in the interaction point of the two high-luminosity experiments ATLAS and CMS. Other type of losses such as injection losses, losses during ramp and squeeze are therefore not considered in the calculation, since their contribution to activation can be assumed negligible with respect to collision losses, and the generated high energy secondary radiation field, during stable beams. However, those losses might be the dominant source term in other points of the machine, e.g. in the collimation regions of IR3 and IR7 or the beam-gas interactions in the arc. The contributions from losses of the beam directed towards the interaction point (IP) and beam-gas interactions are not considered.

An up to date FLUKA model, also including the new HL-LHC galleries, was used to update existing RP studies. Both horizontal crossing (IP1) and vertical crossing (IP5) schemes were simulated. New/updated elements were included in the simulations, such as the latest design of the TAXN shielding, the full model of the crab cavities and the DFX. DPMJET-III [8] was used as the event generator. Results were normalized accordingly to the forecast operation conditions (peak luminosity and integrated luminosity) shown in Figure 1-8 of Ref. [9], referring to the so called “ultimate HL-LHC parameters”. These operation conditions represent the worst-case scenario in terms of radiation protection constraints. Therefore, an ad-hoc FLUKA irradiation profile was built in order to model the HL-LHC operation, as shown in Figure 19-1.

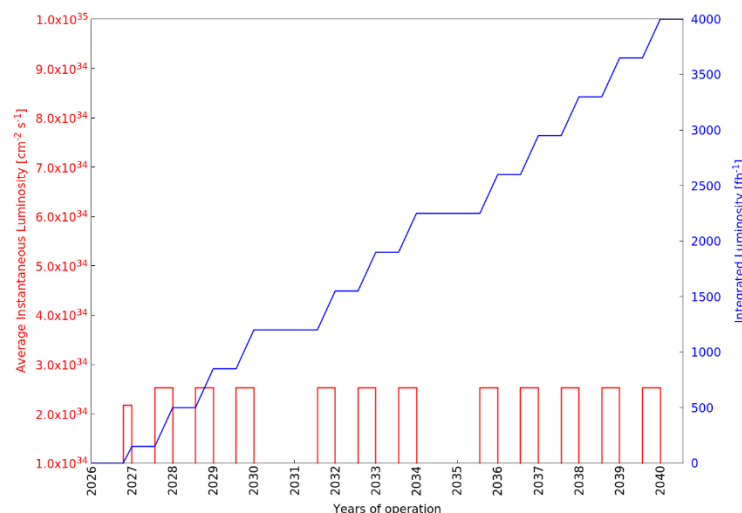


Figure 19-1: Assumed (worst-case) irradiation profile for the HL-LHC operation.

The irradiation profile assumed 160 days of proton-proton physics and a total integrated luminosity of  $4000 \text{ fb}^{-1}$  over the entire lifetime of the HL-LHC machine: an average integrated luminosity of  $350 \text{ fb}^{-1}$  per year was assumed and the average instantaneous luminosity was calculated, assuming an inelastic p-p cross-section of  $80 \text{ mb}$  [10]. The very last 12 hours were assumed to consist of a fill with the maximum levelled luminosity (accordingly to Figure 1-8, [9]) to be conservative for short-lived radionuclides [11]. In addition, two Long Showdowns (LS) of a duration of one year were assumed, namely LS4 and LS5.

As mentioned above, three-dimensional residual dose rate maps were calculated for the entire area from around 14 m distance from the interaction point up to around 270 m distance (i.e. from the TAXS to Q7). The coverage of the 3D mesh included also additional areas, such as ULs, UJs, UPRs, RRs. Six different cooling times were considered covering all typical intervention scenarios: 1 hour, 1 day, 1 week, 4 weeks (assumed equal to one month), 4 months, and 1 year after the last HL-LHC operational period. To give examples for the available results, residual dose rates are reported in the following as two-dimensional maps for a one-month cooling time as well as 1D-profile plots for four different cooling times (1 week, 1 month, 4 months, and 1 year). The values correspond to the average over 40 cm around the beam pipe height ( $y = 0$ ) and, for the 1D-profile plots, between 40–50 cm distances from the outer surface of any equipment on the tunnel side (on average,  $x = -100$  cm from the machine axis, i.e.  $x = 0$ ).

Figure 19-2 shows the ambient dose equivalent rate maps after one month of cooling time during the first Long Shutdown during the HL-LHC era, LS4, in LSS1 (upper plot) and in LSS5 (bottom plot). Both plots refer to the right side of the LSS: while close to the beam line ( $x = \pm 100$  cm) the dose rate maps are symmetric with respect to the IP, differences can be appreciated only in the ULs, UJs and UPRs, and particularly for Point 5 due to the asymmetric infrastructure layout of the UJs. The detailed maps for both left and right side can be found in Ref. [12]. The main difference in between the two ambient dose equivalent rate maps of Figure 19-2 is due to the different crossing angle plane, as well as the different infrastructure layout for what concerns the side alcoves and tunnels.

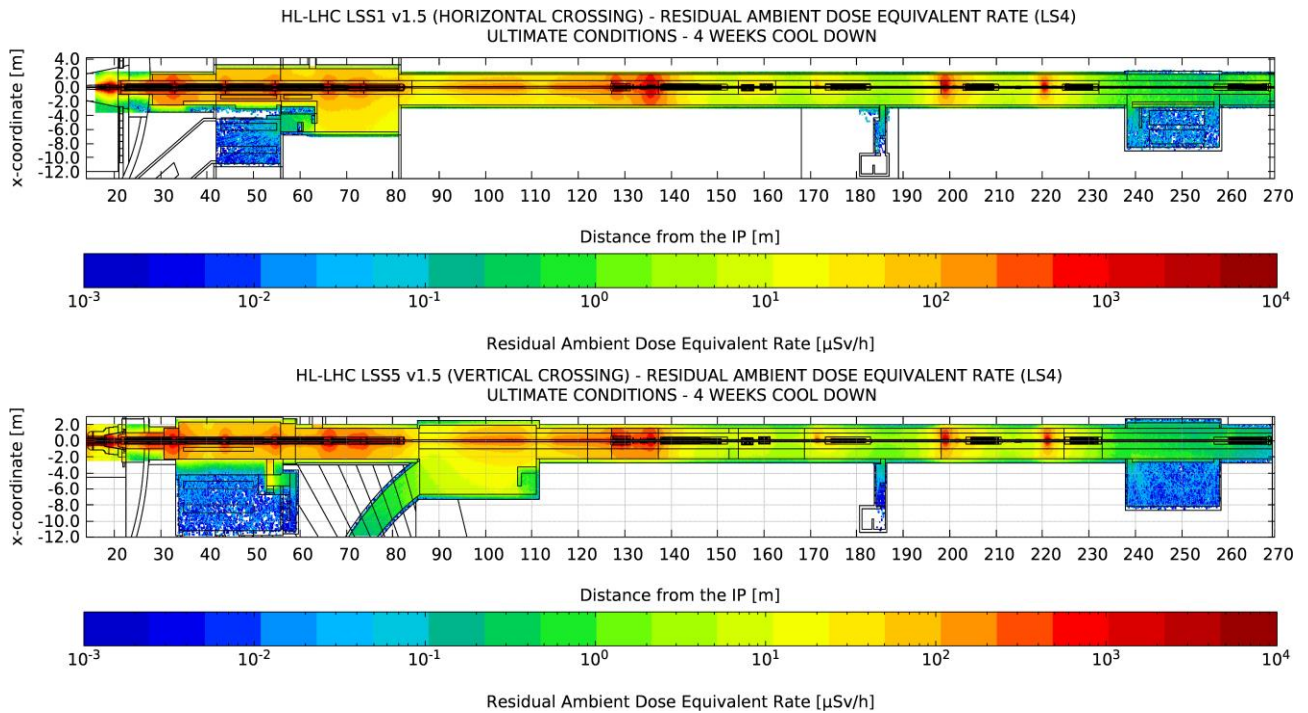


Figure 19-2. Ambient dose equivalent rate maps in the LSS1 (top plot) and in LSS5 (bottom plot) after one-month cooling time during LS4 (ZX plane). The residual dose in the vertical dimension is averaged on 40 cm around the beam pipe ( $y = 0$ ). The highest dose levels are reached (from left to right) at the TAXS, the Inner-Triplet, the TAXN, and the TCL collimators.

Figure 19-3 shows the ambient dose equivalent rate profile in the aisle at a working distance from the machine elements ( $\sim 40$  cm from the outer surface) at four different cooling times: these cooling times are considered as reference for maintenance interventions in the machine tunnel during the scheduled technical stops, end of the year technical stops and long shutdowns. The higher residual dose rates are typically around the elements closest to the IP, such as the inner triplet, and corresponding to the connections between elements, where the shielding effect due to self-absorption of the element is less effective. In addition, high residual dose rates can be found in correspondence of the TAXN and the TCLX collimators. As shown in Figure 19-3, in

case of horizontal crossing, the TCLX4 plays a significant role in protecting the downstream elements, becoming the most active object in the LSS1.

Figure 19-4 shows the radiation level calculated for LSS5. The main difference from the LSS1 values in Figure 19-3 comes from the different crossing scheme in IP5 and, consequently, the different losses on the TCLX4. The inner triplet region shows comparable levels.

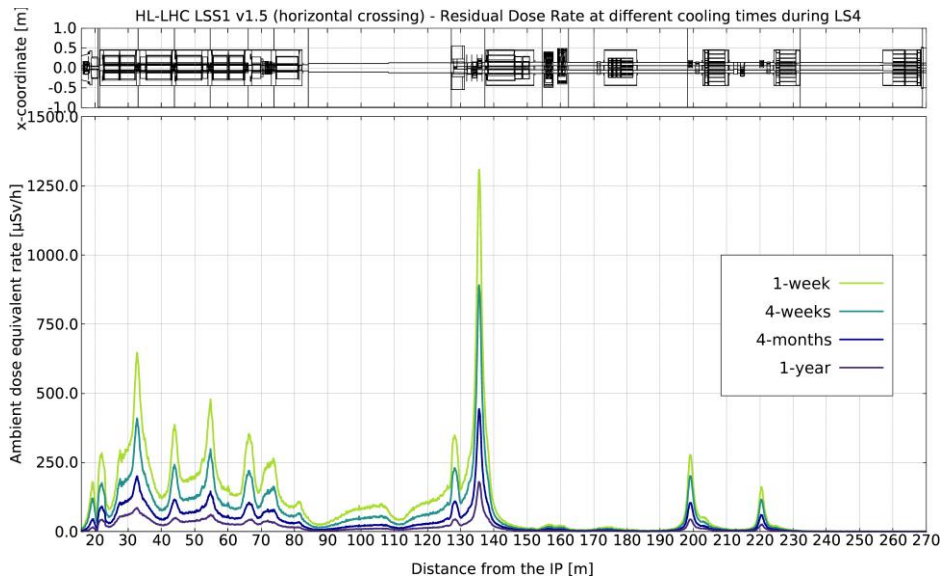


Figure 19-3: Ambient dose equivalent rate profile in the LSS1 at different cooling times during LS4 (z-coordinate). The values correspond to the average over 40 cm around the beam pipe height ( $y = 0$ ) and between 40–50 cm distances from the outer surface of any equipment on the tunnel side (on average,  $x = -100$  cm from the machine axis, i.e.  $x = 0$ ).

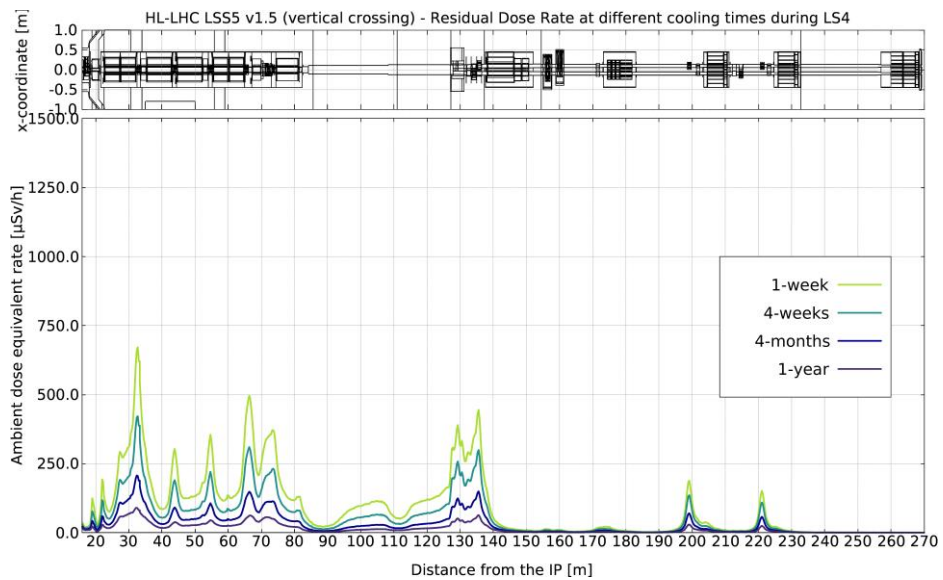


Figure 19-4: Ambient dose equivalent rate profile in the LSS5 at different cooling times during LS4 (z-coordinate). The values correspond to the average over 40 cm around the beam pipe height ( $y = 0$ ) and between 40–50 cm distances from the outer surface of any equipment on the tunnel side (on average,  $x = -100$  cm from the machine axis, i.e.  $x = 0$ ).

### 19.2.3 Radiological risk assessments for the new underground infrastructures in Points 1 and 5

Access to the new US, UR and UA service galleries is foreseen during beam operation (See Chapter 15). For this reason, the radiological impact of the machine operation on the personnel has to be assessed. The UL galleries will be closed during the machine operation, apart from one, in which the first 12 m will be accessible. Two radiological risks have been addressed and will be described here after: air activation and stray radiation.

Risks due to activated air can be either due to direct activation of air inside the new infrastructures by stray radiation or due to streaming of activated air from the LHC tunnel into the new service areas. While the former is expected to be negligible the latter is prevented by static and dynamic confinement of the LHC tunnel air with ventilation doors and ventilation schemes that ensure a lower pressure in the LHC tunnel.

Stray radiation levels will impact the radiological classification of the new service areas. It is foreseen to classify them as Supervised Radiation Areas, similar to any other service area of the LHC. Two different scenarios have been studied, stray radiation during normal operation of the machine and an accidental scenario, represented by one full 7 TeV proton beam lost in a bulky object in front of the most exposing connection to the galleries. The ultimate luminosity and beam intensity are considered ( $7.5 \times 10^{34} \text{ cm}^{-2} \text{ s}^{-1}$  and 2808 bunches at  $2.2 \times 10^{11}$  protons per bunch).

The dose limits follow from the radiological classification as Supervised Radiation Area. During normal operation of the accelerator, in the new service galleries the ambient dose equivalent rate has to be as low as reasonably possible (ALARA principle) and, in any case, it has to be lower than  $15 \mu\text{Sv/h}$ , the limit for non-permanently occupied workplaces. In the accident scenario, the effective dose received by personnel must not exceed the legal annual limit for the class B radiation worker, i.e. 6 mSv.

A standalone geometry model (Figure 19-5), updating the one reported in Ref. [13], of these galleries was developed and used for the shielding studies, such as the choice of the material for the stairs [14]. The model includes the UR and the UA service galleries including the UPR connections, the UA elbow on top of the LHC tunnel with 5 connection cores, and a portion of the LHC tunnel where a tungsten target (100 cm long, 10 cm diameter) is placed in front the UPR-LHC to simulate the accidental loss of the full 7 TeV proton beam on a massive element.

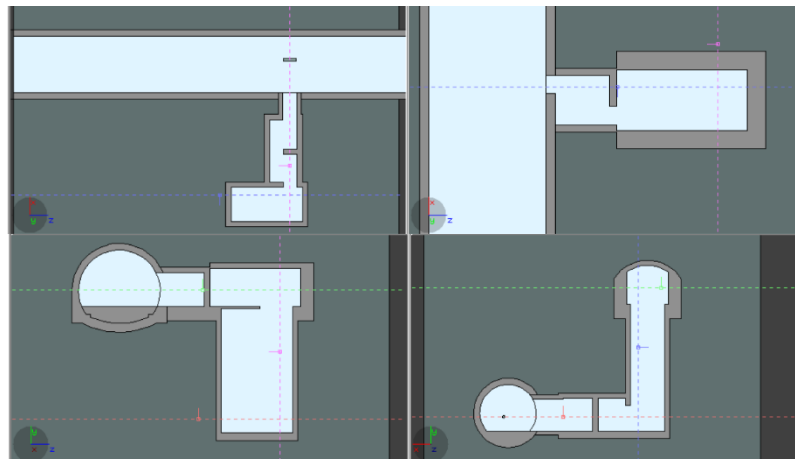


Figure 19-5. Different sections of the FLUKA model of the UPR17. Top-left: top view LHC tunnel-UPR17; Top-right: top view UPR17-UA17 junction; Bottom-left: side view UPR17-UA17 junction; Bottom-right: side view LHC tunnel-UPR17 junction. The stairs are not visible in these sections. A dedicated FLUKA input file has been created for the UPR13, UPR57 and UPR53.

In order to reduce the radiation streaming through the cores connecting the UA elbow to the LHC, two concrete shielding walls are placed at the end of the UA gallery next to the UA elbow. These two walls will be 40 cm thick with a sliding door allowing access to the elbow when the accelerator machine is not operating.

In the following, as example, only the results for the UPR17 are reported. The results for the others UPRxx can be found in Ref. [14]. Figure 19-6 and Figure 19-7 show the ambient dose equivalent maps at the UPR17-LHC and UPR17-UA17 interface respectively. The transmission through the implemented infrastructure, from the LHC tunnel to the closest accessible area in the new UA17 gallery (UPR17-UA17 interface), is estimated to about  $3 \times 10^{-8}$ , where the ambient dose equivalent level drops to  $< 0.3$  mSv (Figure 19-8).

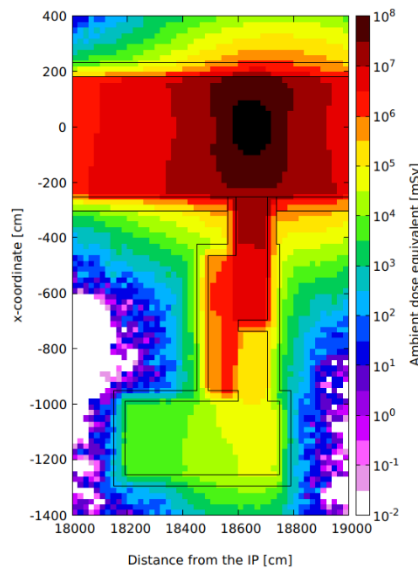


Figure 19-6. Prompt ambient dose equivalent maps for the UPR17-LHC interface considering the full loss of the 7 TeV proton beam on a massive element ( $2808 \times 2.2 \times 10^{11}$ ).

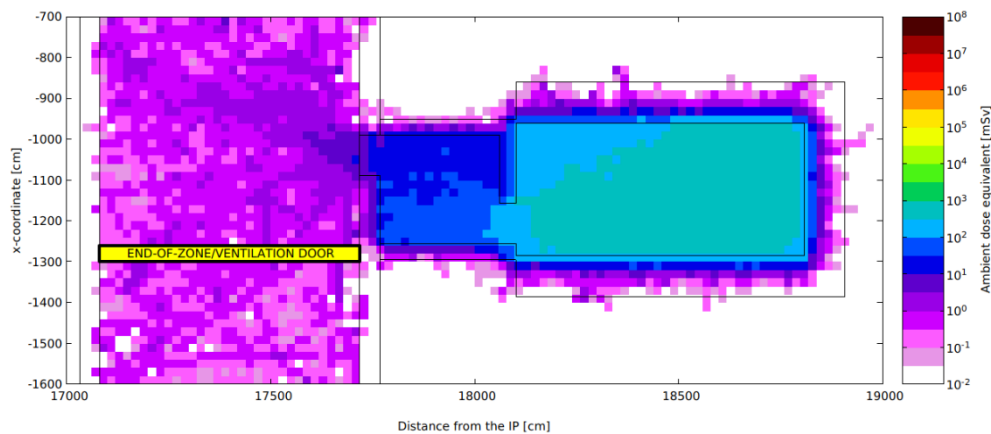


Figure 19-7. Prompt ambient dose equivalent maps for the UPR17-UA17 interface considering the full loss of the 7 TeV proton beam on a massive element ( $2808 \times 2.2 \times 10^{11}$ ).

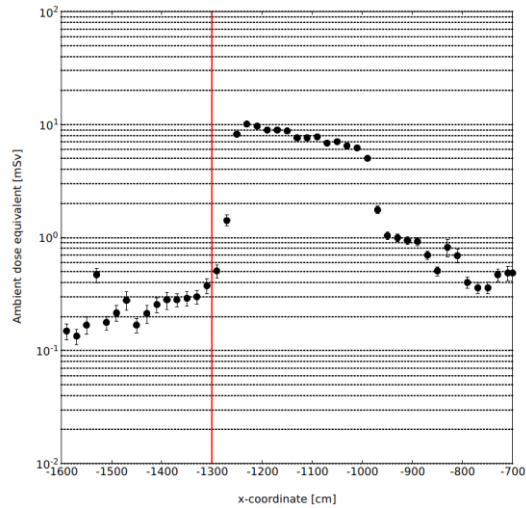


Figure 19-8: Prompt ambient dose equivalent profile along the UA17 tunnel for the full 7 TeV proton beam being lost ( $2808 \times 2.2 \times 10^{11}$ ). The red line indicates the approximate location of the end-of-zone door. Ambient dose scored at 40 cm from the door.  $\Delta y = 300$  cm,  $\Delta z = 600$  cm.

During machine operation, the maximum dose rate next to the tunnel wall is 50 Sv/h, which after applying the attenuation factor of  $3 \times 10^{-8}$ , leads to a value of 1.5  $\mu$ Sv/h ambient dose equivalent rate due to stray radiation in the closest accessible point of the new underground gallery.

19.2.4 Activation studies for the excavation of the new underground galleries in P1 and P5

In order to assess the level of activation of the spoil coming from the excavation of the new underground galleries, the results obtained with the FLUKA Monte Carlo code (particle fluence spectra) have been used as input for the ActiWiz3 Creator © code.

An activated material is defined as radioactive if the specific or total activity of any radionuclides of artificial origin exceed the corresponding clearance limit, i.e.:

$$\sum_{i=1}^n \frac{a_i}{LL_i} < 1 \tag{19-1}$$

where  $a_i$  is the specific activity (Bq/g) or the total activity (Bq) of the  $i^{\text{th}}$  radionuclide of artificial origin in the material,  $LL_i$  is the respective CERN clearance limit for the radionuclide  $i$  in the material and  $n$  is the number of radionuclides present.

During last end of the year technical stop of the LHC machine, some concrete and rock samples were extracted from the LHC tunnel wall, in the place where the excavation will occur.  $\gamma$ -spectrometry measurements were performed on the rock and concrete samples, after a cooling time of about 3 months. The activation of the samples was also evaluated using ActiWiz3 Creator code. The results are reported in Table 19-1, in the form of the sum of specific activity over clearance limit.

Table 19-1: Activation level of concrete and soil samples as measured by the  $\gamma$ -spectrometry and calculated using the ActiWiz3 Creator© code.

| $\sum_i \frac{a_i}{LL_i}$ | 3 months cooling time              |                   |               |
|---------------------------|------------------------------------|-------------------|---------------|
|                           | $\gamma$ spectrometry measurements | ActiWiz3 Creator© |               |
| UPR                       |                                    |                   | only $\gamma$ |
| concrete                  | 1.15E-01                           | 9.70E-02          | 4.96E-01      |
| soil                      | 8.17E-03                           | 5.30E-03          | 1.65E-02      |

In the last column of Table 19-1, the results of all the radionuclides is reported, including the ones that cannot be measured with the  $\gamma$ -spectrometry technique. The  $\gamma$  results, second and third column Table 19-1, are in good agreement. The induced radionuclide list calculated is reported in Table 19-2 with the contributing percentages to the sum; the most contributing radionuclide in both cases is Ca-45, which is a pure  $\beta$ -emitter, thus not measurable with the  $\gamma$ -spectrometry technique.

The activity over limit sum was evaluated for the spoils coming from the excavation of the new underground galleries where they are connected to the existing LHC tunnel. The results of the calculation, for the first three meters of excavation spoils is reported in Figure 19-9, for one and four months cooling times; the first meter of excavated spoils will be radioactive, the second and the third meters are below the legal limits in both the cases.

Table 19-2: Contributing percentage of the induced radionuclide

|              | Contribution to $\sum_i \frac{a_i}{LL_i}$ | Contribution to $\sum_i \frac{a_i}{LL_i}$ |
|--------------|---|---|
| Radionuclide | Concrete sample                           | Soil sample                               |
| Ca-45        | 80%                                       | 68%                                       |
| Na-22        | 7%  | 28%                                       |
| Zn-65        | 3%  |   |
| Fe-55        | 3%  |   |
| S-35         | 1%  | 2%  |
| Mn-54        | 1%  |   |

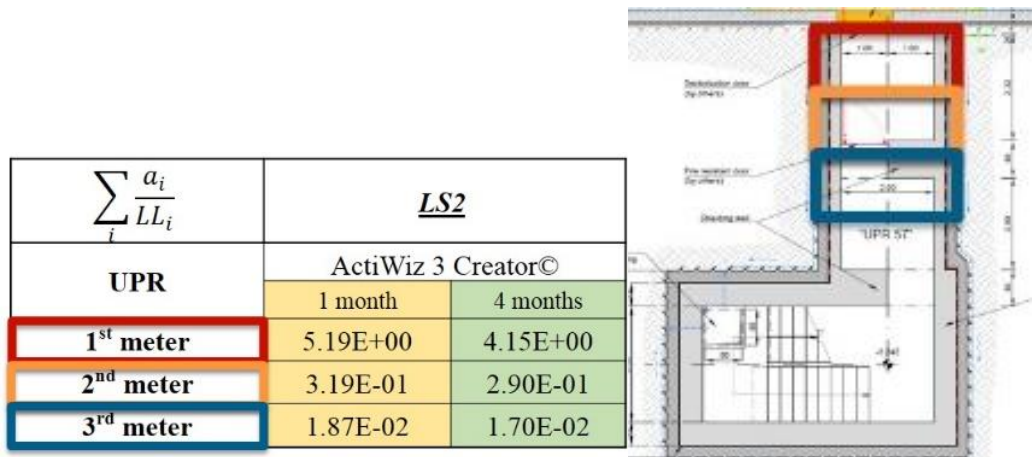


Figure 19-9: Expected activation level of excavated spoils.

### 19.2.5 Preliminary residual dose rate prediction for the Long Straight Section in Point 8

A preliminary activation study, considering the LSS left of IP8, has been performed to give guidelines for the design of the new neutral absorber, TANB (See Chapter 8). Different design options have been evaluated, with and without shielding. Figure 19-10 shows the FLUKA geometry model and the TANB model used for the study.

Residual dose rate maps were calculated with FLUKA for the part of LSS in Point 8 that extends from the warm dipole MBXWH on the left of IP8 up to the dipole D2 in Cell 4 left. As for P1 and P5, the simulations were performed for the high energy secondary radiation field arising from p-p collisions at 14 TeV centre-of-mass energy as it dominates the activation in these areas. Results were normalized to the nominal LHC peak luminosity value of  $2 \times 10^{33} \text{ cm}^{-2} \text{ s}^{-1}$ , using DPMJET-III as the event generator. The irradiation profile considered was based on the operational scenarios reported in Ref. [1] and consists in two operational runs (Run 3 and Run 4) of three years each, at nominal peak luminosity and a total integrated luminosity per run of  $25 \text{ fb}^{-1}$  with a composition of  $5 \text{ fb}^{-1}/10 \text{ fb}^{-1}/10 \text{ fb}^{-1}$  over the three operational years of each run.



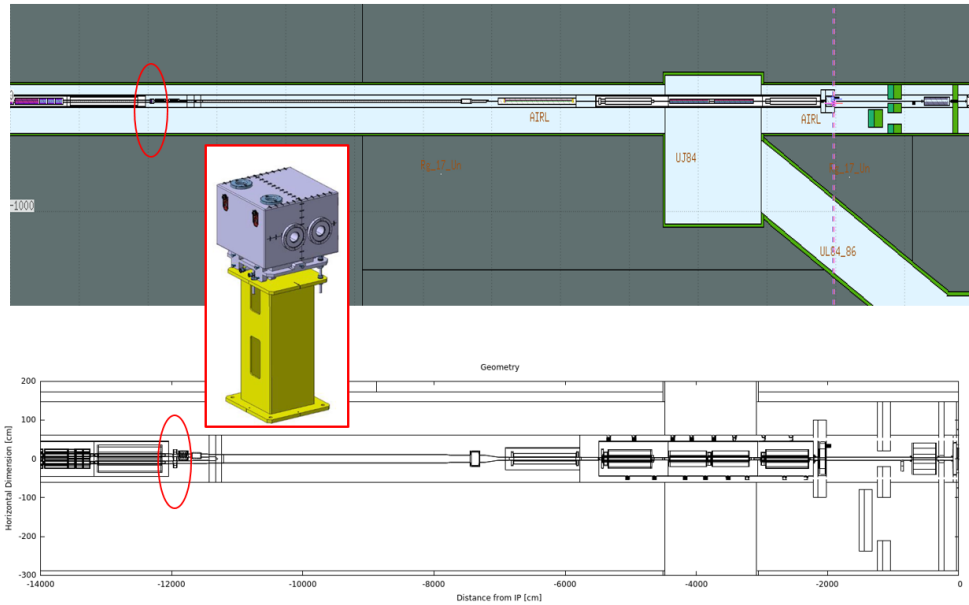


Figure 19-10. FLUKA geometry model of the LSS left of IP8 and the TANB model.

Figure 19-11 shows the ambient dose equivalent rate map after one month of cooling time during the LS3, and Figure 19-12 shows the ambient dose equivalent rate profile in the aisle at a working distance from the machine elements at four different cooling times (1 week, 1 month, 4 months and 1 year), which are typical cooling times for maintenance interventions in the machine tunnel during the scheduled technical stops, end of the year technical stops and long shutdowns. The higher residual dose rates are around the elements closest to the IP (elements on the right in the figures) where the highest levels in the aisle correspond to the connections between elements, where the shielding effect due to self-absorption of the element is less effective, and in cell 4 where there is the Y chamber, the TCT collimators and the TANB absorber.

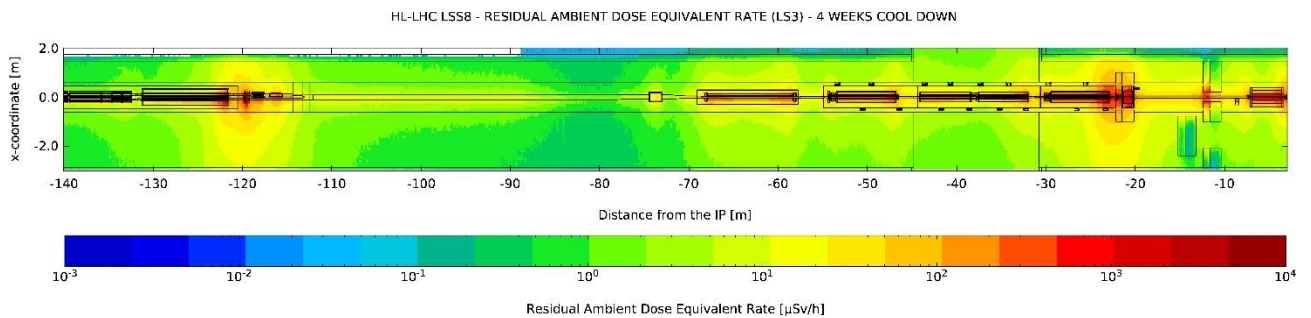


Figure 19-11. Ambient dose equivalent rate map in the LSS8 left after one-month cooling time during LS3. The residual dose in the vertical dimension is averaged on 30 cm around the beam pipe.

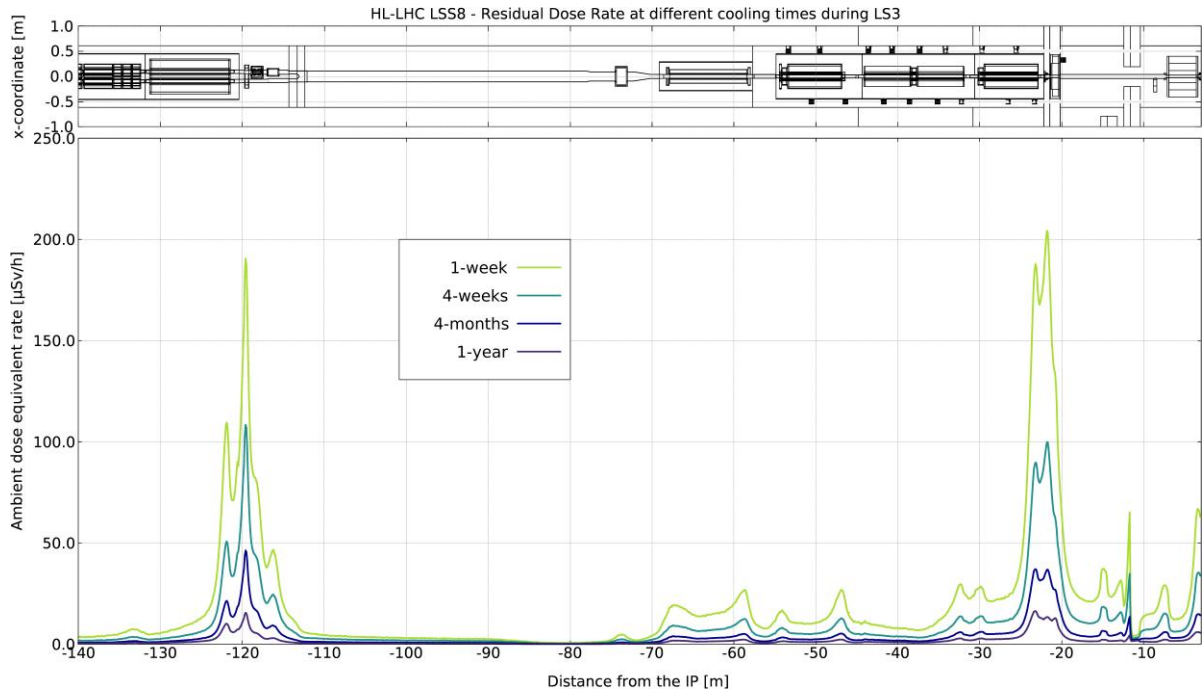


Figure 19-12. Ambient dose equivalent rate profile in the LSS8 left at different cooling times during LS3. The residual doses in the horizontal and vertical dimensions are averaged on 30 cm.

Figure 19-13 shows the ambient dose equivalent rate profiles in the aisle at a working distance from the TANB and adjacent equipment corresponding to three different material shielding options of the absorber: stainless steel, cast iron, marble and without shielding. The advised design option is the one without shielding.

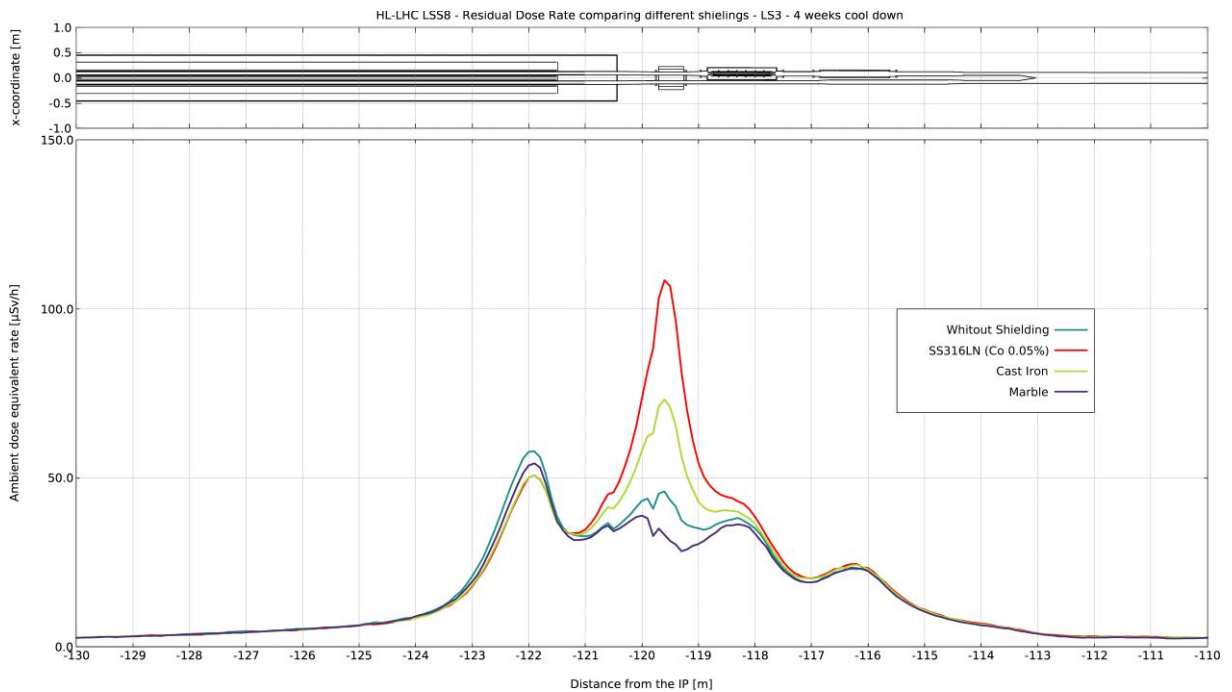


Figure 19-13. Ambient dose equivalent rate profiles around TANB, for different shielding options at 1-month cooling time during LS3. The residual doses in the horizontal and vertical dimensions are averaged on 30 cm.

### 19.3 Occupational, Operational, Radiation Safety, and Safety Conformity

#### 19.3.1 Introduction

Safety of a facility can be highlighted from different perspectives: first, there is a temporal distinction between the project phase, the operational phase and later the decommissioning phase. Second, one can distinguish between the conformity aspect of Safety (the project's deliverables shall comply with Safety regulations, standards and recommendations), the aspects of workplace safety (the prevention of professional accidents and professional illness by instructing, training and protecting workers), and operational safety (definition and approval of technical and organisational measures to ensure a safe operation of a facility), including radiation safety.

This Section highlights the strategies developed to ascertain compliance of the HL-LHCs hardware with Safety Standards and regulations. Workplace safety is not particular to the HL-LHC project, but part of the hierarchical responsibility of the executive departments and units.

#### 19.3.2 Project safety at CERN

A project pools together resources from numerous, specialised organisational units from all over CERN in a Matrix structure in order to achieve its objectives. A specific organisation is put into place for projects, including the project's Safety aspects [16]. The project leader assumes responsibility for the Safety of the Project, however, neither he, nor the Project organisation substitute the Hierarchical Line of Safety Responsibility that is mandatory at CERN [1][18]. The organisational units participating in the project retain responsibility for results, both technical and in matters of Safety. An example is the delivery of accelerator components, meeting applicable safety standards, and best safety practice during their production. The project's responsibility is the provision of the necessary means to meet the technical and safety objectives, in form of manpower, budgets and a common safety organisation.

In a larger project, the project leader is advised to appoint a Project Safety Officer (PSO) [16][18] to assist him with his Safety responsibilities.

The central Health, Safety and Environmental Protection (HSE) unit has the role to establish a regulatory framework for Safety within CERN, to advise organisational units and projects on its implementation, and to monitor the installation of special equipment and activities by safety clearances and inspections.

The Departmental Safety offices are already involved during the project phase, so that they can advise on the design and operational aspects. Indeed, the risk owners remain the Departments which is particularly true as soon as the project organisation stands down at the beginning of the operational phase.

#### 19.3.3 Safety documentation

The decisions taken on behalf of Safety during the project phase need to be documented and archived properly for future lifecycle phases of the equipment built under the HL-LHC project. One of the PSO's tasks is therefore to oversee the edition of the Safety Documentation, in parallel with the project's development. In this function, the PSO collaborates closely with the work package leaders and project engineers, and with members of the HSE unit (HL-LHC HSE Correspondents and HSE experts).

For the HL-LHC project, it has been decided to create a safety documentation that follows the project breakdown structure. The safety documentation is recorded in the System Safety Assessment (SSA) form, with a content agreed between the project and the HSE unit. The SSA form is a living document, accompanying the equipment during the life cycle, after which it will be archived with the equipment's documentation. The aim is that during the operational phase of the equipment, this document is updated for each modification so that the hazards and risks can be re-evaluated regularly. The SSA for each equipment or assembly is archived under the "Safety" heading in the Workpackage's EDMS space. Safety documents pertaining to individual assets

(e.g. one specific magnet from the series) are stored with the asset's technical documentation in the Equipment Management Folder (MTF) database.

The first step of the safety documentation consists in the production of a hazard register, between a Project Safety Officer and the Work Package Leader and engineers [17] and based on an agreed table of potential hazards [19]. Targeted hazards are those that may appear during installation, operation, maintenance, and dismantling of the equipment. For many hazards, "standard best practice" from CERN safety regulations or national rules or recommendations can be applied to suppress them. The hazard register and the mitigation measures are recorded in the SSA and submitted for review to the HSE unit. The HSE unit may accept it, and then the Project Safety Officers will monitor the implementation of the mitigation measures by the Work Packages. Where standard best practice is not sufficient to mitigate a hazard, the HSE unit may decide that the equipment has "Major Safety implications (mSi)". Based on the hazard register and the risk assessment, the HSE unit will finally define "Safety Checks" which have to be fulfilled before the equipment receives "Safety Clearance" and can be installed and operated in the accelerator.

Equipment or systems with "major safety implications" include deliverables from collaboration partners that are external to the EU and thus not able to certify conformity with EU directives as well as equipment employing novel technologies not documented in the safety literature, such as the crab cavities or the cold powering system. In these cases, a dedicated risk assessment will be performed by the Project Safety Officers in collaboration with the work package leader and engineers. It is documented either in the SSA or in a dedicated safety report. Examples are given below. Other risks requiring dedicated analysis and reporting are those which may lead to helium release and oxygen deficiency.

### 19.3.4 Conformity with safety standards

The likelihood of equipment failure leading to an accident or occupational illness is reduced by installing only equipment that meets published Safety regulations and standards. These regulatory documents draw on the pooled experience in workplace safety of panels of experts working on behalf of the public authorities. CERN has adopted the Essential Safety Requirements (ESR) of the European Directives as the safety standard for its technical equipment. These requirements are met by an equipment that is constructed following the applicable Harmonised European Norms (EN), technical standards, but the compliance can also be achieved by other means.

Other sources of Safety regulations and standards may be national regulations of a Host State, or specific regulations at CERN, which are published in form of a Safety Regulation (SR) or a General Safety Instruction (GSI) [20].

### 19.3.5 Examples - superconducting magnets, cold powering and crab cavities

Two HL-LHC WPs will produce superconducting magnets, based either on Nb<sub>3</sub>Sn or Nb-Ti conductor technology. WP11 provides 11-T superconducting magnets produced at CERN. WP3 is relying on contributions from partners in Italy, France, Spain, U.S.A., Japan, and China. The cold masses of superconducting magnets are pressure vessels. Their safety is ascertained world-wide by legal prescriptions, backed by mandatory industrial standards. They differ in certain details from the prescriptions in the European Directives and harmonised standards. It would be prohibitively expensive in terms of budget and time to assess conformity of their contributions with European Standards, and this assessment would not add significantly to the quality and the safety of the equipment received. It has therefore been agreed upon between the project and the HSE unit to deviate in this aspect from a strict adherence to the European Safety Directives. The HSE unit will act as a de facto Notified Body with regard to the assessment of the conformity of the deliverables to the ESR. On the basis of an inspection checklist [21] drawn up by the project and the HSE unit that sets out the minimum requirements relating to the equipment, the HL-LHC HSE Correspondents make an evaluation if the conformity assurance methods put in place by countries using other standards are suitable to meet the Essential Safety Requirements of the European Directive. It may decide compensatory measures throughout the lifecycle of the equipment to proceed with the next steps of manufacture if necessary. Documents to be delivered for

the Safety Checks are described in Ref. [21]. The roles and responsibilities of the manufacturer, the importer and the HSE unit are precisely defined within a formal agreement written and signed by the three parties [22].

The high-current magnets in the HL-LHC inner triplets and in part of the matching section are powered from the new underground galleries by a superconducting link. The link is made from a MgB<sub>2</sub> superconducting cable, cooled by gaseous helium. The advantage of this scheme is that the feedboxes hosting the current leads are not exposed to ionising radiation (which is the case of present LHC DFBX and DFBM) and that they can be inspected during the operation of the accelerator. The price to pay is, however, that a fully powered, superconducting system is partly installed in an accessible part of the underground structures. A feedbox in the accessible service tunnel will make the link between busbars or water-cooled cables and the superconducting MgB<sub>2</sub> cable. This cable will be guided in a superconducting link cryostat of up to 90 m length to the LHC tunnel. There, a second feedbox will make the electrical connection to the superconducting magnets. The cold powering will rely on European In-kind contributions to manufacture the interconnection cryostats which are pressure vessels. The EU manufacturer will choose the conformity assessment process according to the category level of the equipment and deliver it to CERN with an EU certificate of conformity with the stamp of the nominated Notified Body. Once the interconnection cryostats are delivered to CERN, the HSE unit will make a complementary conformity assessment before connecting pipes and assembling the equipment in the tunnel.

A failure mode and effects analysis (FMEA) has identified the maximum credible incidents (MCI) of the cold powering system. The information from this analysis is used in the design process of the safety devices (pressure relief valves and burst disks) which must assure that only the limited amount of gaseous helium contained in the link cryostat can be released to the accessible parts of the underground galleries during an MCI [23]. The outcome of this study will also be used to define and implement other technical protection and organizational measures to ensure a safe operation of the superconducting link when work is simultaneously being performed in the accessible service galleries (e.g. deflectors, ventilation, and maintenance procedures).

WP4 provides Crab Cavities to the project, RF devices which improve the overlap of the proton bunches in the interaction points and thus increase luminosity. They present several challenges for Safety compliance: the cavities are cryogenic devices and therefore pressure vessels, constructed from the non-standard material Niobium. In addition, some of the deliverables are supplied by non-EU countries. Similar to the procedure outlined for superconducting magnets, an approval process for this non-standard equipment was defined with the HSE unit, which defined a number of Safety Checks in order to grant clearance for the Crab Cavities. This process was applied to the first prototype of a Double Quarter Wave cavity, which was successfully tested in the SPS accelerator in 2018.

#### 19.4 References

- [1] CERN, “CERN Safety Policy”, EDMS: [1416908](#).
- [2] CERN, “CERN Safety Code F”, EDMS: [335729](#).
- [3] CERN, “ALARA rule applied to interventions at CERN”, EDMS: [1751123](#).
- [4] CERN, “ALARA Review Working Group. Final report”, 2013. EDMS: [1244380](#).
- [5] C. Theis and H. Vincke, “ActiWiz – optimizing your nuclide inventory at proton accelerators with a computer code,” in Proceedings of the ICRS12 conference, 2012, Nara, Japan, Progress in Nuclear Science and Technology, Volume 4 pp. 228-232, 2014, DOI: [10.15669/pnst.4.228](#).
- [6] A. Ferrari, P.R. Sala, A. Fassò, and J. Ranft, “FLUKA: a multi-particle transport code”, 2005, DOI: [10.5170/CERN-2005-010](#).
- [7] T. Böhlen, F. Cerutti, M.P.W. Chin, A. Fassò, A. Ferrari, P.G. Ortega, A. Mairani, P.R. Sala, G. Smirnov and V. Vlachoudis, “The FLUKA Code: Developments and Challenges for High Energy and Medical Applications,” Nuclear Data Sheets 120, 211-214, 2014, DOI: [10.1016/j.nds.2014.07.049](#)

- [8] S. Roesler, E. Enge and J. Ranft, The Monte Carlo Event Generator DPMJET-III, Vols. in Proceedings of the Monte Carlo 2000 Conference Lisbon, October 23-26, A. Kling, F. Barao, M. Nakagawa, L. Tavora and P. Vaz, Eds., Springer-Verlag Berlin, 2001, DOI: [10.1007/978-3-642-18211-2\\_166](https://doi.org/10.1007/978-3-642-18211-2_166)
- [9] G. Apollinari, I. Bejar Alonso, O. Bruning, P. Fessia, M. Lamont, L. Rossi and L. Tavian, High Luminosity Large Hadron Collider (HL-LHC): Technical Design Report V.0.1., 2017, DOI: [10.23731/CYRM-2017-004](https://doi.org/10.23731/CYRM-2017-004)
- [10] Csörgő, T. *et al.*, “Elastic Scattering and Total Cross-Section in p+p reactions measured by the LHC Experiment TOTEM at  $\sqrt{s} = 7$  TeV,” in XLI International Symposium on Multiparticle Dynamics, 2012, DOI: [10.1143/PTPS.193.180](https://doi.org/10.1143/PTPS.193.180)
- [11] V. Kouskoura and R. Froeschl, “Radiological Source Terms for the FIRIA ATLAS Pilot Case,” CERN, Geneva, 2020.
- [12] A. Infantino and M. Maietta, “Radiation levels in HL-LHC LSS1 and LSS5: update to optics v1.5, EDMS: [2405113](https://cds.cern.ch/record/2405113).
- [13] C. Adorisio, “HL-LHC - Residual Dose Rate Estimations in the LSS1 and LSS5 (from TAXS up to Q7)”, EDMS: [1868872](https://cds.cern.ch/record/1868872).
- [14] A. Infantino, “HL-LHC UPR underground galleries: review of the ambient dose equivalent rate during operation”, EDMS: [2212147](https://cds.cern.ch/record/2212147).
- [15] E. Thomas, “LHCb request for running at 'nominal' LHC luminosity”, 5<sup>th</sup> Joint HiLumi LHC-LARP Annual Meeting, 2015, INDICO: [400665](https://indico.cern.ch/event/400665).
- [16] CERN, “Safety Regulation SR-SO "Responsibilities and Organisational Structure in Matters of Safety at CERN", EDMS: [1389540](https://cds.cern.ch/record/1389540).
- [17] T. Otto and F. Viggiano, “Hazard Classification for Technological processes in TE Department”, EDMS: [1586444](https://cds.cern.ch/record/1586444).
- [18] CERN, “General Safety Instruction GSI-SO-7”, EDMS: [1410233](https://cds.cern.ch/record/1410233).
- [19] CERN, “HL-LHC Hazard Identification Table”, EDMS: [1361970](https://cds.cern.ch/record/1361970).
- [20] CERN, “Safety Procedure SP-R1 “Establishing, updating, and publishing CERN Safety Rules”, EDMS: [872057](https://cds.cern.ch/record/872057).
- [21] CERN, HSE, “HL-LHC requirements for Cat IV pressure equipment”, EDMS: [2087591](https://cds.cern.ch/record/2087591).
- [22] CERN, “Agreement for compliance of LMBXF cold masses supplied by KEK with CERN Safety Rules”, EDMS: [2052040](https://cds.cern.ch/record/2052040).
- [23] T. Otto and N. Grada, “Preliminary Assessment of the Cryogenic Releases from Cold Powering in HL-LHC Underground Areas”, EDMS: [1974133](https://cds.cern.ch/record/1974133).